Protocol for Optimal Size Selection of Punched Screen in Steam Assisted Gravity Drainage Operations

Chenxi Wang [a], Jesus D. Montero Pallares [a], Mohammad Haftani [a], Alireza Nouri [a]

[a] *Department of Civil & Environmental Engineering and the School of Mining & Petroleum Engineering, University of Alberta, AB, Canada*

Abstract

Punched screen as a stand-alone screen is gaining more and more popularity in Steam Assisted Gravity Drainage (SAGD) operations. However, the literature contains limited studies for proper aperture size selection and the performance of the punched screen. This paper aims at investigating the performance of punched screen and generating an aperture size selection protocol for SAGD production wells.

In this study, pre-packed sand retention tests (SRT) are conducted to analyze the screen performance by using punched screen coupons. These tests incorporate several influential factors, including particle size distribution (PSD), flow velocity, and aperture size, into the performance analysis. Sanding and flow performance are the two governing factors for the size selection protocol. The sanding performance guides the upper limit of the safe size window, and flow performance indicates the lower limit. Therefore, the optimal size window is determined to obtain desirable sanding and flow performance. In this paper, the size selection protocol is illustrated to show the optimal size window of the punched screen.

This paper presents an optimal size selection protocol for SAGD production wells. The protocol can be used by SAGD operators to obtain the proper aperture size for punched screen to maximize production rates and profits.

Key Words: Punched Screen, SAGD, Size Selection Protocol, Graphical Window.

1. Introduction

SAGD has been used as a useful technology for the heavy oil recovery of unconsolidated oil-bearing sands in Canada (Butler and Stephens, 1981; Butler, 1985; Butler, 2001; Gates et al., 2005; Zhang et al., 2007). In SAGD operations, two horizontal wells with 500 to 1,200 meters length are drilled. The vertical distance between the horizontal well pair is around five meters (Butler, 1998; Nasr et al., 1998; Dang et al., 2010). Steam is injected into the upper injection well to reduce the bitumen viscosity. Melted bitumen will be produced from the lower production well. Figure 1 shows the schematic view of SAGD wells and the steam chamber.

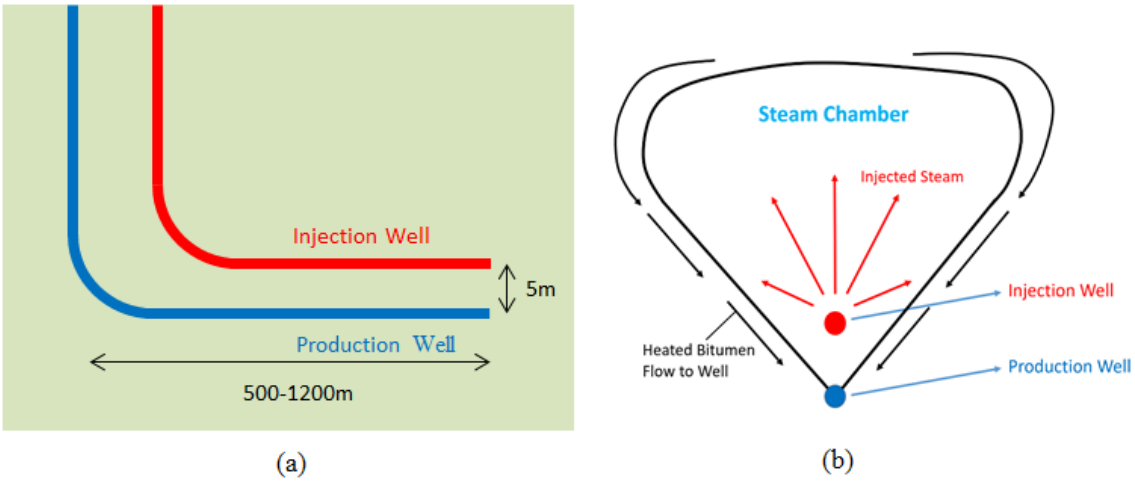

Fig. 1 Schematics of SAGD (a) well positioning (b) and steam chamber.

Sand production is a crucial issue for unconsolidated formations under thermal exploitation (Yi, 2002; Han et al., 2007; Dong et al., 2014; Anderson, 2017; Ma et al., 2018; Ma et al., 2019a). The produced sand may damage pipelines, pumps, and other facilities. Severe sand production can even plug the production tubing and cause costly remediation. (Al-Awad et al., 1999; Denney, 2008; Sanyal et al., 2012). Stand-alone screens are usually applied in SAGD production wells to prevent sand production and maintain effective and long-term liquid production. (Bennion et al., 2009; Romanova et al., 2014; Xie, 2015; Mahmoudi et al., 2016b; Montero Pallares et al., 2018b; Wang et al., 2018). Slotted liner, wire-wrapped screen, and punched screen (PS) are the three typical stand-alone screen types. The punched screen has been used in the heavy oil recovery process as the completion tool (Naganathan et al., 2006; Zhang, 2017). Recently, the punched screen is gaining popularity in the SAGD operation due to its relatively high open-flow-area (OFA) (3-8%) and low cost (Matanovic et al., 2012; Spronk et al., 2015; Fattahpour et al., 2018). In punched screens, a punched stainless-steel filtration jacket is welded onto a carbon-steel perforated based pipe. The stainless-steel jacket provides a strong resistance to corrosion, and the base pipe ensures mechanical integrity. The trapezoid-shape aperture geometry alleviates the plugging issues (Zhang, 2017). Figure 2 shows the configuration of the PS and the schematics of its slot geometry.

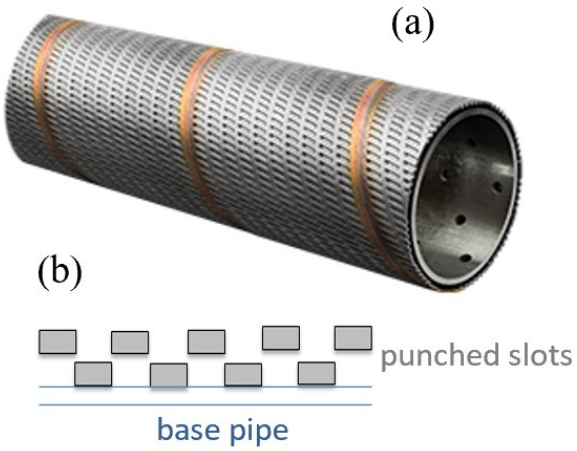

Fig. 2 (a) An image of a PS (RGL Reservoir Management Inc, 2018), and (b) schematics of PS slot geometry

Aperture size design is a crucial factor for stand-alone screens. Proper aperture size selection is the key to achieving a desirable sanding and flow performance for the stand-alone screen for the entire SAGD life (Bennett et al., 2000; Bennion et al., 2009; Xie, 2015). Coberly (1937) suggested that the screen opening size should be smaller than two times the D_{10} (the sieve size at which 10% of the sample's mass consists of particles with a diameter larger than this value) of the formation sand. However, this and similar criteria have not been developed for PS, particularly for SAGD conditions.

The optimal aperture size can be obtained from sand control tests. Slurry SRT and pre-packed SRT are commonly used in the industry to assess the optimal aperture size of stand-alone screens (Ballard and Beare, 2006; Constien and Skidmore, 2006; Williams et al., 2006; Bennion et al., 2009; Chanpura et al., 2012a; Romanova et al., 2014; Devere-Bennett 2015; O'Hara 2015; Dong et al., 2016; Mahmoudi et al., 2016b; Anderson 2017; Ma et al., 2019b; Wang et al., 2020a).

In slurry SRT, slurry with low sand concentration (less than 1% of volume) is pumped into a cell and flow towards the screen. This test replicates a gradual sand erosion around the borehole (Gillespie et al., 2000; Underdown et al., 2001; Ballard and Beare, 2006; Williams et al., 2006; Mathisen et al., 2007; Chanpura et al., 2012b). In pre-packed SRT, the sand sample is packed onto a screen coupon to emulate the case in which the annulus between the screen and wellbore has fully collapsed. Pressure readings and sand production are two major measurements obtained during the pre-paced SRT (Ballard and Beare, 2006; Williams et al., 2006; Mathisen et al., 2007; Chanpura et al., 2012b).

In SAGD, during the pre-heating stage, the sand around the borehole contacts with the hot steam. Hence, the bitumen as the bonding material melts, resulting in the collapse of the oil sands on the screen, creating a high-porosity zone. Thus, the pre-packed SRT has been agreed to properly represent the SAGD wellbore condition (Ballard and Beare, 2006; Constien and Skidmore, 2006; Williams et al., 2006; Bennion et al., 2009; Chanpura et al., 2012b; Romanova et al., 2014; Devere-

Bennett 2015; O'Hara 2015; Spronk et al., 2015; Anderson 2017; Wang et al., 2020a). Some criteria have been proposed for the optimal aperture size design from the pre-packed SRT. These criteria have been developed based on the maximum acceptable sand production for SAGD production wells, which is between 0.12 and 0.15 lb/ft^2 (Hodge et al., 2002; Chanpura et al., 2011). Retained permeability (RP) is proposed by Chanpura et al. (2011) and Mahmoudi et al. (2018) to assess the flow performance of stand-alone screens. The RP is defined as the ratio of screen permeability over the initial permeability of the sand-pack. The screen permeability considers the formation permeability in the near-screen zone and the screen. The minimum and marginally acceptable level for the flow performance have been proposed to be 50% and 70% of retained permeability (Hodge et al., 2002; Mahmoudi et al., 2018). The optimal size design should meet both the sanding and flow performance criteria.

In this paper, the optimal aperture size selection protocol for PS in SAGD production wells was obtained through pre-packed SRT tests. The protocol is presented graphically by using the traffic light system (TLS) approach (Mahmoudi 2017; Mahmoudi et al. 2018; Wang et al., 2020a). The TLS uses colour codes to identify the safe aperture window. The protocol incorporates reservoir and operational conditions, fluid conditions, and flow rates into the size selection analysis. The following sections introduce the testing facilities, testing design, and the results of the TLS size selection protocol for the punched screen.

2. Experimental Investigation

2.1 Pre-packed SRT Setup

Figure 3 shows the schematics and an image of the multi-phase flow pre-packed SRT testing facility used in this study. This apparatus consists of six main components: 1) fluid injection unit, 2) sand-pack cell, 3) data acquisition system (LabVIEW), 4) screen coupon, 5) sand production measurement unit, and 6) back-pressure column.

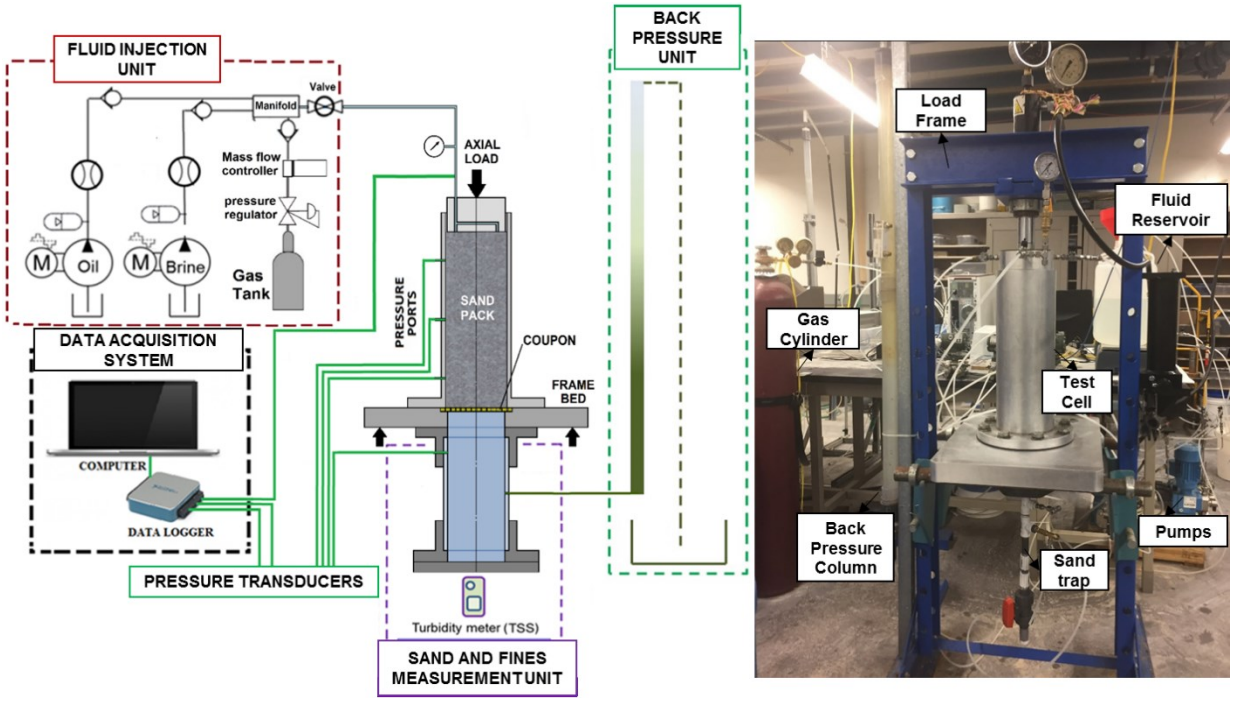

Fig. 3 Schematics and an image of the multi-phase flow SRT setup

The sand-pack cell is 16.5 inches in height and accommodates a 6 inches PS coupon in diameter. Three differential pressure transducers (0.25% full-scale accuracy) associated with LabVIEW are connected to measure the pressure difference along the sand-pack sample during the test. The first pressure transducer measures the pressure drop in the bottom section from two inches above the coupon to below the coupon. The pressure drop in the bottom segment is used to calculate the so-called screen permeability. The next two pressure transducers record the pressure difference in the middle and top sections of 5 inches distance (Fig. 3). The fluid injection unit contains one brine pump, one oil pump, and one nitrogen gas cylinder. Brine and oil are injected by two triplex solenoid diaphragm metering pumps, and flow rates are measured by a graduated cylinder (2-cc accuracy). The gas injection rates are controlled by a nitrogen flow meter with 3% full-scale accuracy. Producing fluids flow through the 3-psi back-pressure column and get discharged.

2.2 Testing Material

2.2.1 Sand-pack

The SRT experiments used synthetic sand-pack samples by mixing different types of commercial sands and clay (Mahmoudi et al., 2016a). The reason for using replica samples was their availability, low cost, and repeatability of experiments. The synthetic samples have similar PSD and mineralogy with target formation sands. There are four major PSD categories in the McMurray Formation shown in Fig. 4 (Abram and Cain, 2014).

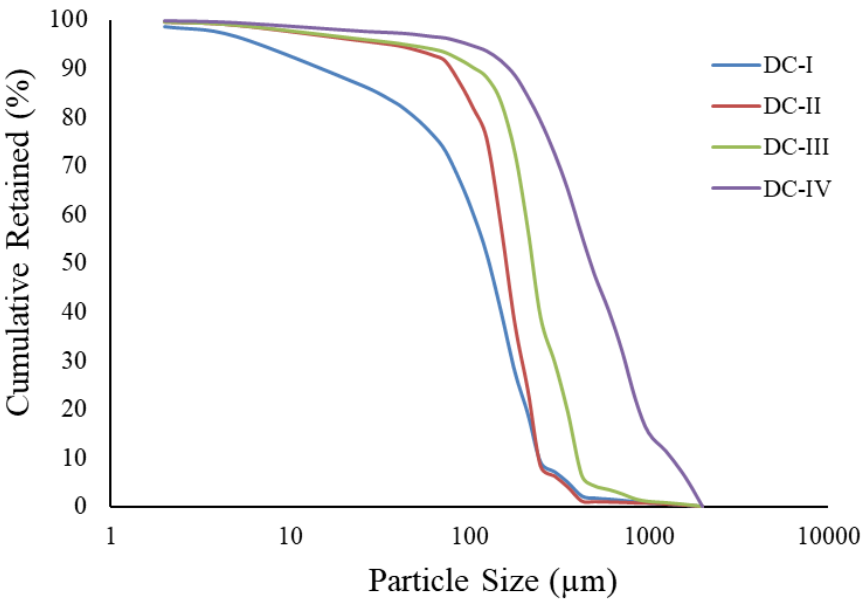

Fig. 4 PSD categories for the McMurray Formation (Abram and Cain, 2014)

This study employed three dominant PSD types (DC-I, II, and III) in the testing design. PSDs of commercial sands, slits, and clay used in the synthetic sample replication process are presented in Fig. 5.

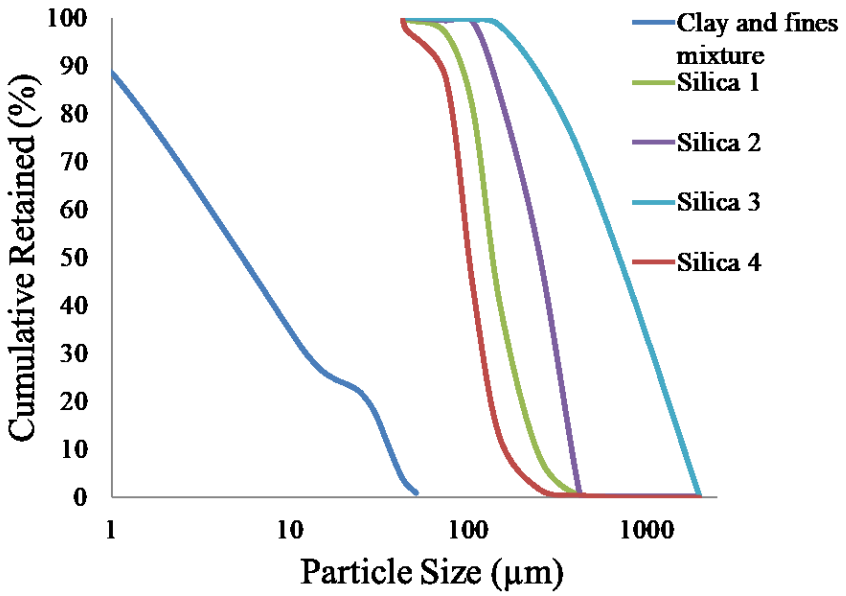

Fig. 5 PSDs of commercial sands, silts, and clays used to synthesize samples

Figures 6-8 show the original and matched PSD's. Kaolinite, as the dominant clay type in the McMurray Formation (Romanova et al., 2015; Mahmoudi et al., 2016a) is used in the synthetic samples.

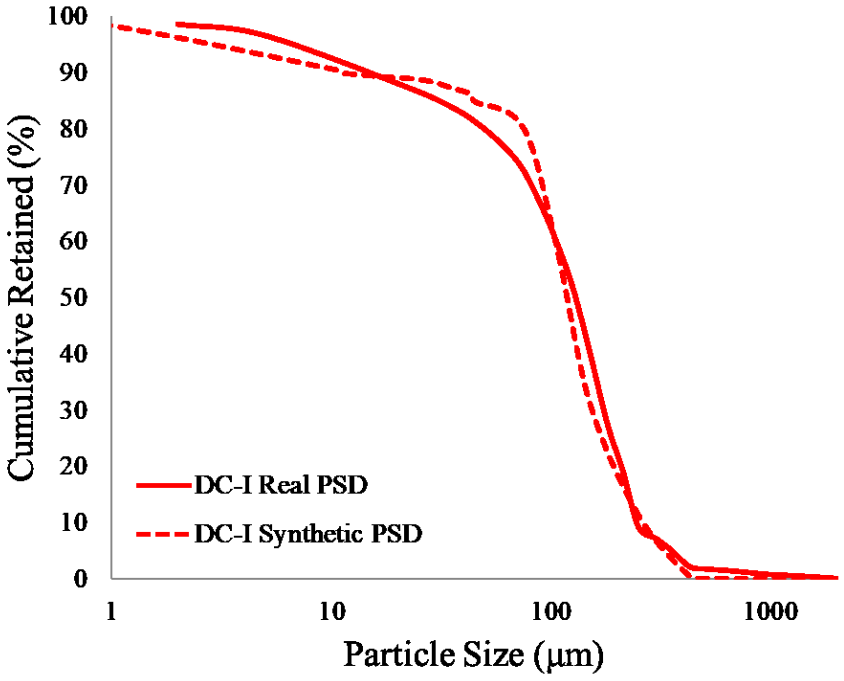

Fig. 6 PSD matching results for DC-I

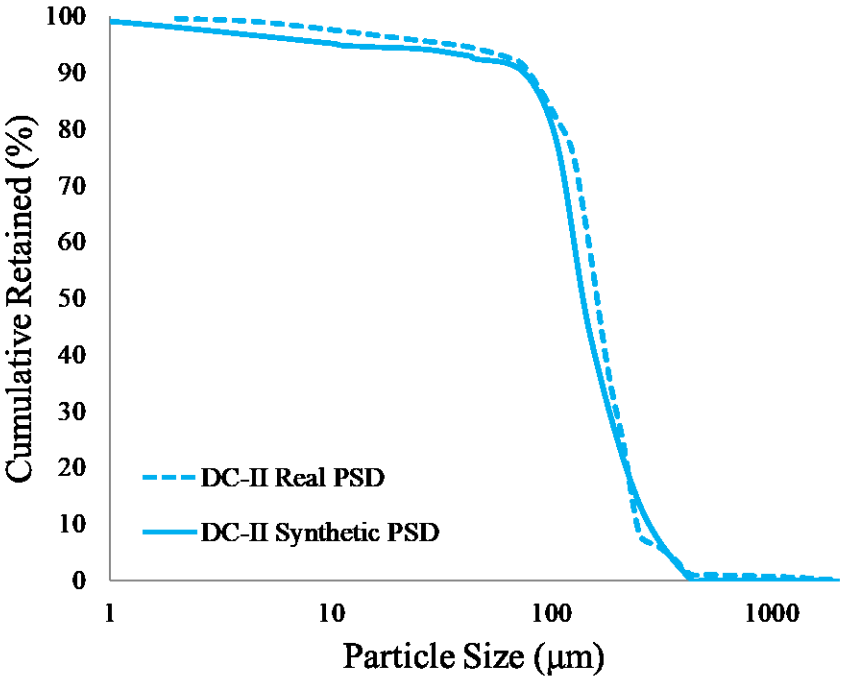

Fig. 7 PSD matching results for DC-II

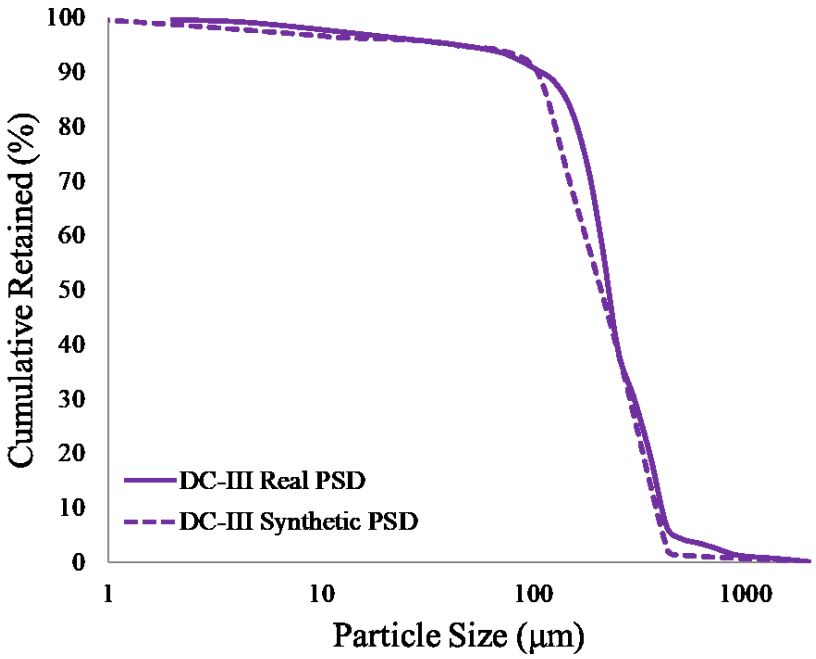

Fig. 8 PSD matching results for DC-III

2.2.2 Flowing Fluids

The Sodium Chloride brine used in tests has a 400-ppm salinity and 7.9 pH. It is reported that the values of 400 ppm for salinity (Minnich et al., 2013) and 7.9 for pH (Cowie et al., 2015; Birks et al., 2017) are within the ranges of SAGD produced water. The salinity of 400 ppm is chosen to create the worst-case scenario for fines migration. Khilar and Fogler (1984) found that there is a critical salt concentration (CSC) for clay particles to release and migrate. Flocculation potential of clay particles increases when the salinity level goes farther (Kotylar et al. 1996).

The oil used in tests is mineral oil. The viscosity of the oil is 8 cp at laboratory temperature (20℃), which represents the actual oil viscosity in the SAGD downhole high-temperature condition (Romanova et al., 2014).

2.2.3. Punched Screen Coupons

PS coupons shown in Fig. 9 are used in the experiments to analyze the screen performance. Table 1 presents the OFA of the punched coupon of different aperture size used in the testing program.

Fig. 9 An image of a punched screen coupon

2.3 Testing Matrix

This study includes nine SRT experiments. Three different aperture sizes are selected for all PSD categories. Table 2 shows the aperture sizes and corresponding OFA.

Table 1 Aperture size and OFA of the tested PS coupons

	Aperture Size (inches)	OFA (%)
PS	0.010	3.7
PS	0.014	5.2
PS	0.019	7

2.4 Testing Procedure

The pre-packed SRT testing procedure includes (1) synthetic sand sample preparation, (2) sample packing, (3) sand-pack saturation, (4) fluid injection, (5) data acquisition and measurement, and (6) SRT cell disassembly. Details of each procedure is stated in Wang et al., (2020b).

The testing starts with fluid injection in three steps: (1) single-phase oil flow (Stages 1-3), (2) two-phase oil and brine injection (Stages 4-8), (3) three-phase oil-water-gas injection (Stages 9-10). Different water cut (WC) levels (50%, 75%, and 100%) are designed in two-phase flow stages to emulate the increase of water cut in the produced liquid due to steam condensation (Noik et al., 2005; Montero et al., 2018). The three-phase brine-oil-gas flow emulates the potential steam breakthrough scenario in SAGD (Fig. 10).

Testing flow rates in Fig. 10 are chosen based on typical production rates in SAGD wells: 4000 bbl/day considering a 600-m and 7-inch-diameter production well (Montero Pallares et al., 2018a; Wang et al., 2020a). The normalized flow rate is around 7400 cc/hr/ft^2. The area of the coupon is 0.196 ft^2. Thus, the basic flow rate scaled down by the coupon area is 1450 cc/hr. Then, the flow rates used in the test design are obtained by applying three different effective flow percentages (50%, 30%, and 20%) to this basic flow rate to account for the increase of flow velocity due to aperture partially plugging and non-uniform flow distribution along the well (Romanova and Ma,

2013). Two gas flow rates are chosen to account for potential steam breakthrough scenarios (Montero Pallares et al., 2018b; Fattahpour et al., 2018).

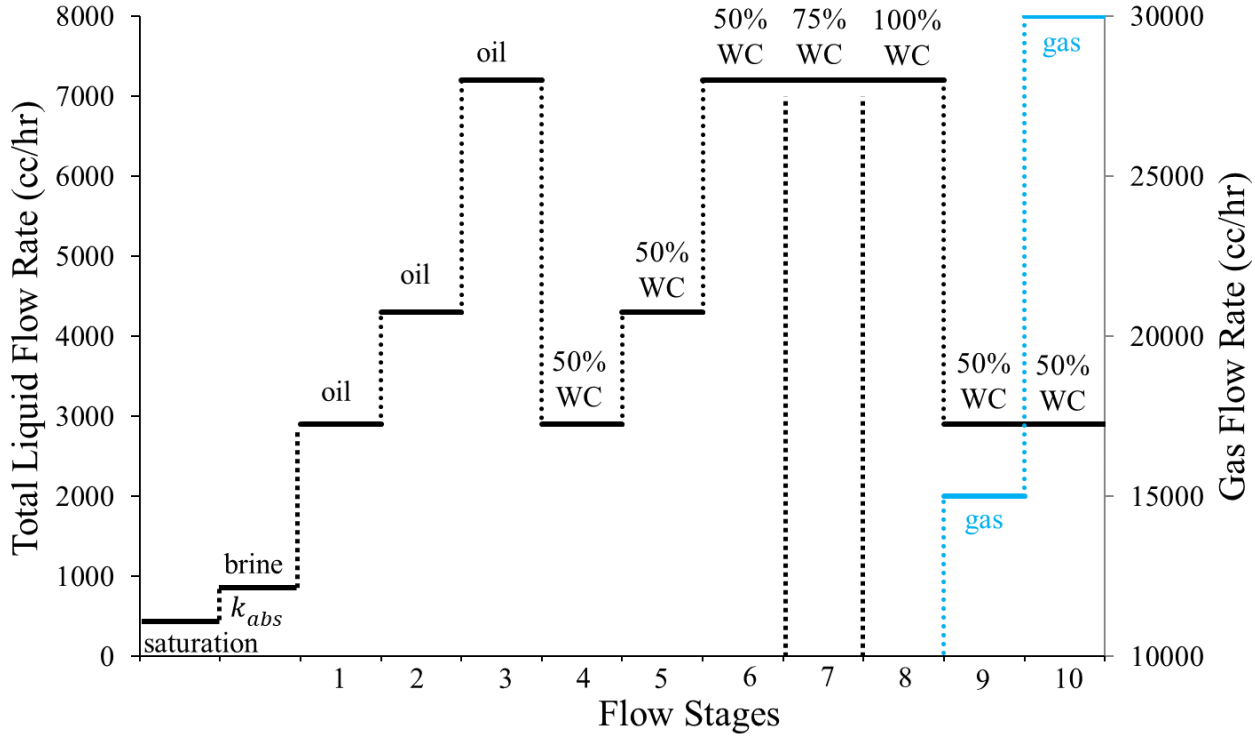

Fig. 10 Flow rates in various stages of the SRTs

3. Testing Results

3.1 Sanding Performance of PS

Figures 11-13 show the cumulative sand production for each flow stage for all three PSD categories. It is found that minimum sand production is observed during the single-phase oil flow stages (Stages 1-3), which can be attributed to the strong capillary bonding force in the system. The capillary bonding acts as a resisting force, which prevents the sand production. However, the amount of sand production increases after water breakthrough (Stage 4) due to the reduction of the capillary force. Moreover, sanding increases with higher flow velocities (Stages 4-6) and water cut (Stages 6-8). The reason is the stronger drag forces at higher flow velocities and weaker capillary force at higher water cuts. Another significant increase in sand production occurs during gas breakthrough (Stages 9-10). The reason is higher flow velocities when water, oil, and gas are concurrently flowing in the sample, causing a stronger drag force on the sand grains, hence, more sand production. Further, the pore pressure in the specimen increases during the three-phase flow, leading to reduced effective stress and weaker friction between the sand grains. The result is increased sand production.

Also, these figures show the acceptable and unacceptable sand production limits (0.12 and 0.15 lb/ft^2) in yellow and red lines. If the cumulative sand production is below 0.12, it is deemed that

the sanding performance is desirable. If the amount is between 0.12 and 0.15, the sanding performance is considered as marginal. The screen fails the sanding performance if the produced sand is over 0.15.

It is found that for DC-I, the aperture size of 0.019'' could not provide desirable sand control performance. The amount of cumulative sand production exceeds the sanding limit during the liquid flow stage. The aperture size 0.014'' shows good sanding performance during liquid flow stage. However, the cumulative sand production exceeds the limit (0.15) during the three-phase flow condition. The aperture size of 0.010'' can provide excellent sand retention capability, although the final cumulative sand production is at the margin of the sanding limit (0.12).

For DC-II and III, all aperture sizes (0.010'', 0.014'', and 0.019'') can provide an excellent sanding performance during liquid flow stages (Stages 1-8). However, when it comes to three-phase flow, the PS with 0.019'' aperture size shows less sand retention capability. The cumulative amount of sand production is over the sanding limit (0.15), which means this aperture size could not provide desirable sanding performance during three-phase flow condition.

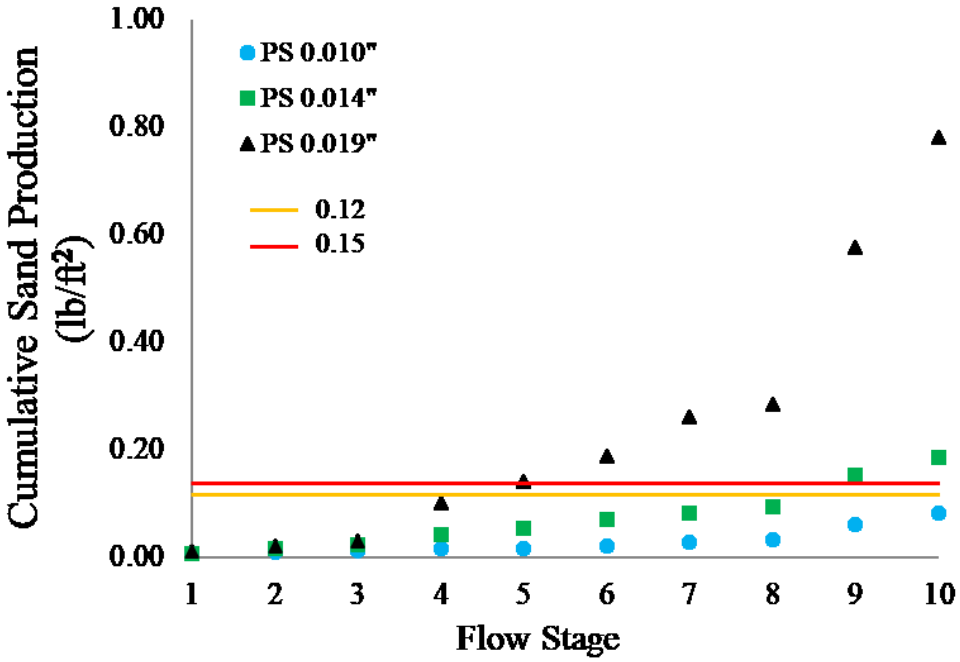

Fig.11 Cumulative sand production for DC-I

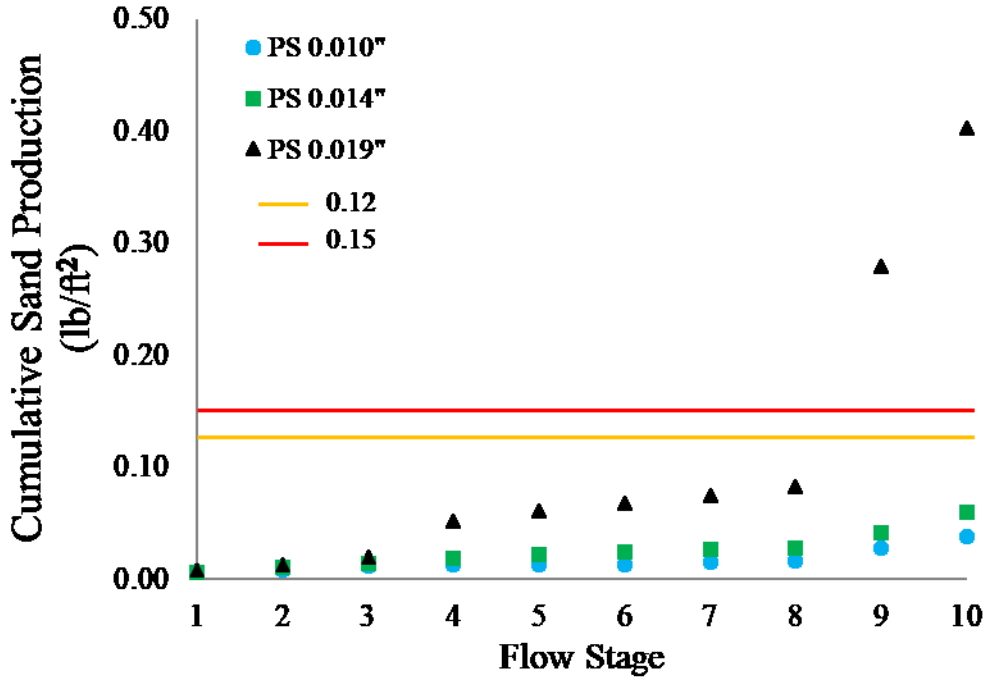

Fig.12 Cumulative sand production for DC-II

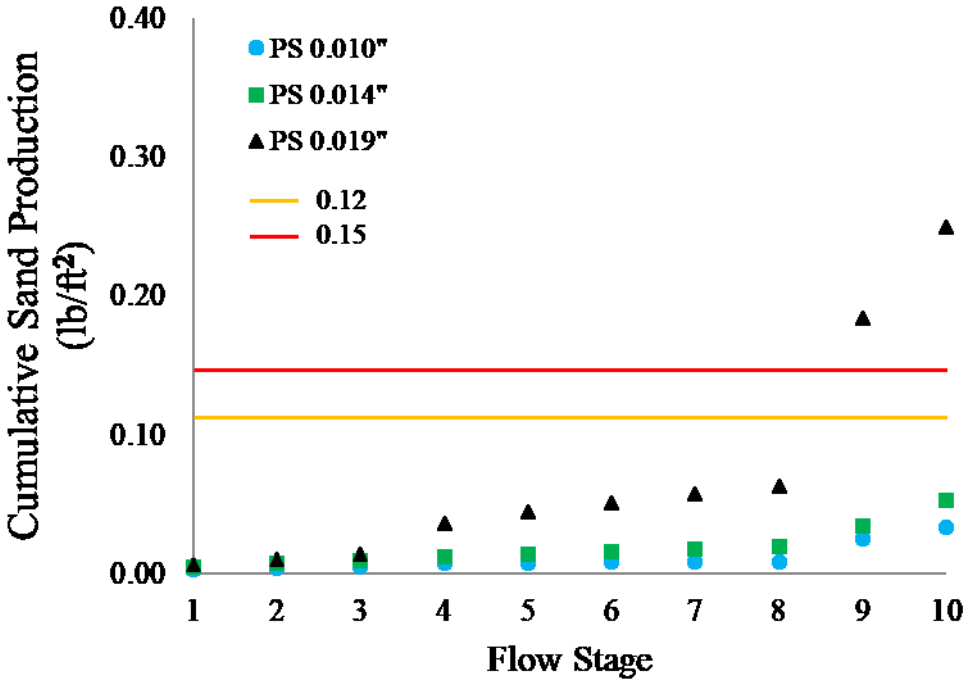

Fig.13 Cumulative sand production for DC-III

3.2 Flow Performance of PS

Wang et al., (2020b) developed a methodology to calculate the retained permeability under multi-phase testing condition. In this paper, the retained permeability is calculated at the final liquid flow stage (Stage 8) to characterize the flow performance. The testing condition of this stage is single-phase (brine) flow at residual oil saturation condition. The water relative permeability values at such conditions for each PSD are measured in separate tests at initial condition. Then, these values are used in the retained permeability calculation. To calculate the retained permeability, first the effective permeability is obtained based on Darcy' Law by using Eq. 1.

$$q_{water} = \frac{k_{eff} \cdot A \cdot \Delta P_{screen}}{\mu_{water} \cdot L} \quad \text{(Eq. 1)}$$

Next, Eq. 2 is used to obtain the absolute permeability value from the effective permeability.

$$k_{abs} = \frac{k_{eff}}{k_{rw@initial\ condition}} \quad \text{(Eq. 2)}$$

Finally, the retained permeability by Eq. 3.

$$RP = \frac{k_{abs}}{k_{abs@initial\ condition}} \quad \text{(Eq. 3)}$$

Table 2 shows the absolute permeability and relative permeability of brine at residual oil saturation for the initial sand-pack condition.

Table 2 k_{abs} and k_{rw} in initial conditions

	DC-I	DC-II	DC-III
k_{abs} (md)	950	1800	2400
k_{rw}	0.48	0.52	0.54

Following the procedures (Eq. 1, 2, and 3), the retained permeability of each PSD is calculated and showed in Table 3.

Table 3 Retained permeability results

	DC-I	DC-II	DC-III
Aperture Size (inch)	RP (%)	RP (%)	RP (%)
0.010	51	61	65
0.014	57	67	71
0.019	65	76	80

From the retained permeability results, it can be concluded that all the aperture sizes can provide satisfactory flow performance for all tested PSD's. However, for DC-I, it should be noted that the flow performance of the PS with an aperture size of 0.010″ is at the margin of the limit value (0.5).

4. Graphical Size Selection Protocol

The aperture size selection protocol is generated based on the testing results: sand production and retained permeability. The protocol is illustrated graphically by using the "Traffic Light System" (TLS). In the TLS, the red, yellow, and green colours represent unacceptable, marginal, and acceptable performance, respectively. The aperture size design criteria in the TLS are based on sanding and flow performance. The sand production controls the upper limit of the aperture window Retained permeability dictates the lower limit. The definitions of colours are summarized in Table 4 (Mahmoudi 2017; Mahmoudi et al. 2018; Wang et al., 2020a).

Table 4 Colour definitions in TLS

Sand production performance	
red	sand production > 0.15 lb/ft^2
yellow	0.12 < sand production < 0.15 lb/ft^2
green	sand production < 0.12 lb/ft^2
Flow performance	
red	retained permeability < 0.5
yellow	0.5 < retained permeability < 0.7
green	retained permeability > 0.7

Also, the D-values of each PSD are used to mark the linear axis to present the safe aperture window as shown in Figures 14 through 16.

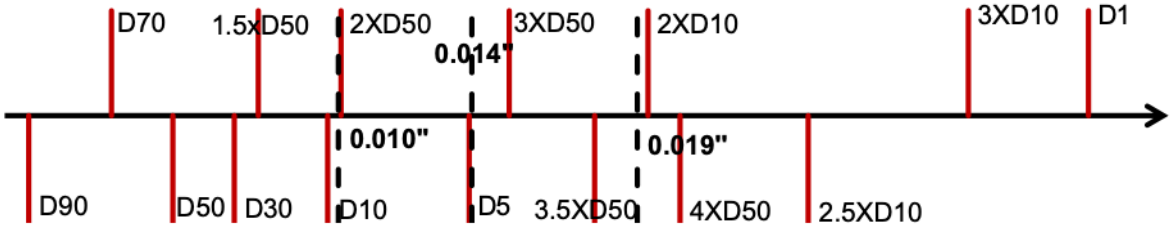

Fig. 14 Linear axis for the presentation of the safe slot window for DC-I PSD

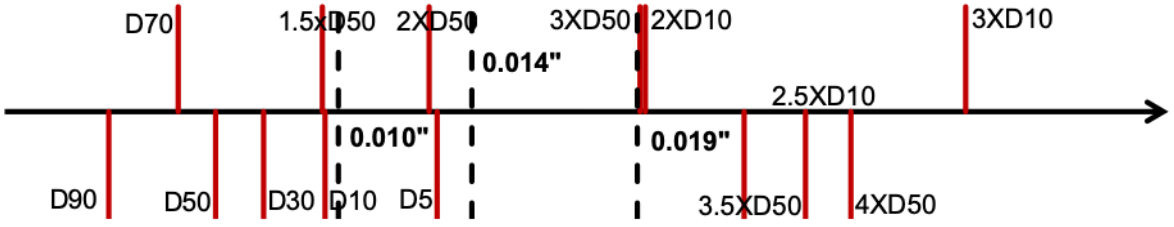

Fig. 15 Linear axis for the presentation of the safe slot window for DC-II PSD

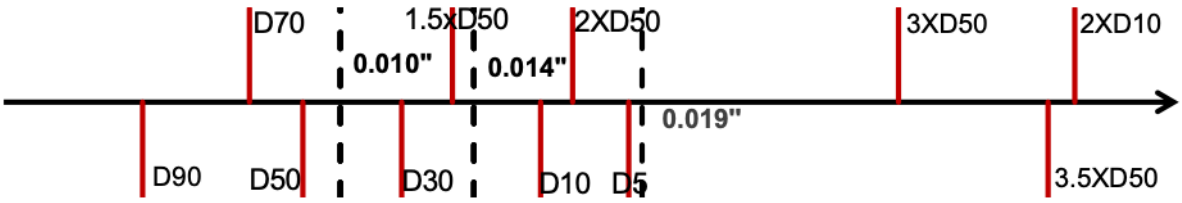

Fig. 16 Linear axis for the presentation of the safe slot window for DC-III PSD

In this protocol, two representative scenarios are considered, namely, normal SAGD condition and aggressive SAGD condition. The normal condition includes only the liquid flow stages (Stages 1-8) while the aggressive condition also includes gas flow stages (Stages 9-10) to account for the potential steam breakthrough.

Figure 17 shows the flowchart for developing the TLS design criteria for PS based on the results of the prepacked SRT experiments for each PSD. Figures 18 to 22 show the details of how the TLS are created based on the sanding and flow performance.

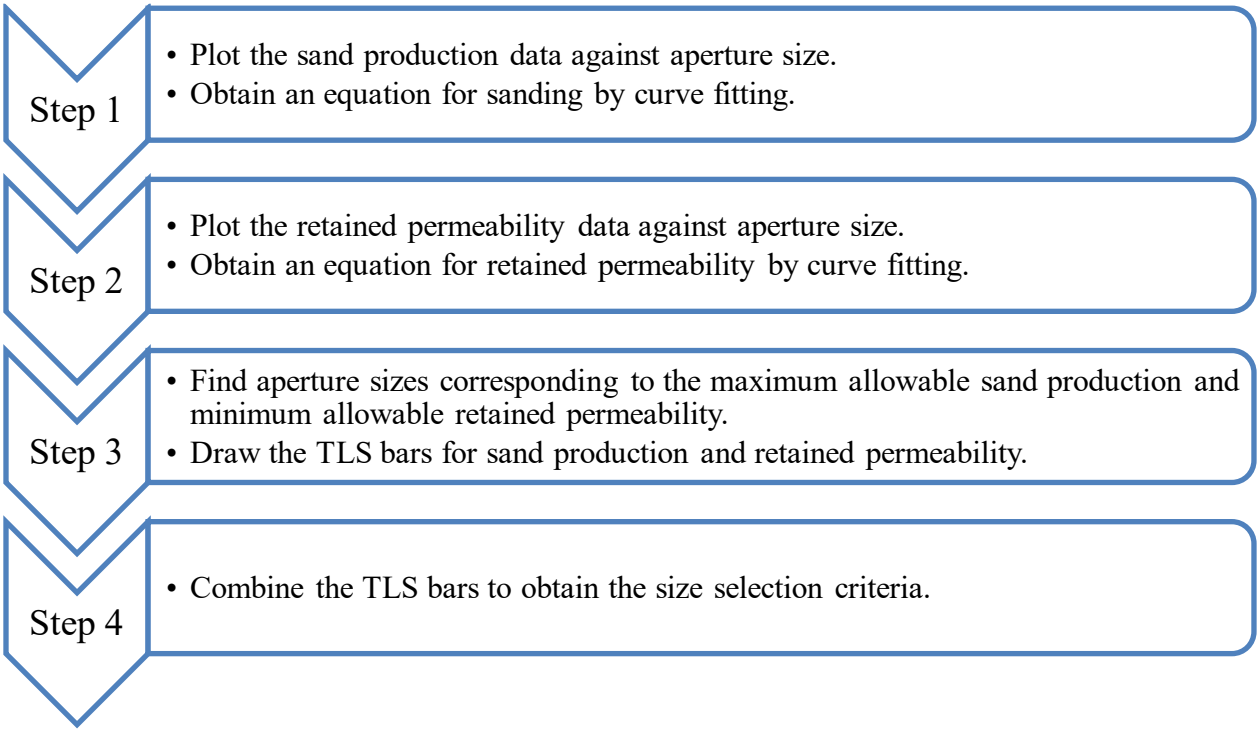

Fig. 17 Flowchart for developing TLS design criteria

The testing results for DC-I (normal condition) are used as an example to explain the development of the TLS criteria in further details. First, the final cumulative sand production and retained permeability results obtained from different tests, are plotted against aperture sizes, as shown in Figures 18, and 19, respectively. Next, mathematical equations that correlate the sand production or retained permeability with the aperture size are obtained by curve fitting. These equations are used to find the aperture sizes that correspond to the acceptable boundaries for the sanding (0.12

and 0.15 lb/ft^2) and flow performance (50% and 70%). Once the appropriate aperture size determined, the TLS bars are separately created for the sand production (Fig. 20) and retained permeability (Fig. 21). Finally, the sand production and retained permeability TLS bars are combined to obtain the overall TLS showing the safe window for aperture size design, as shown in Figure 22.

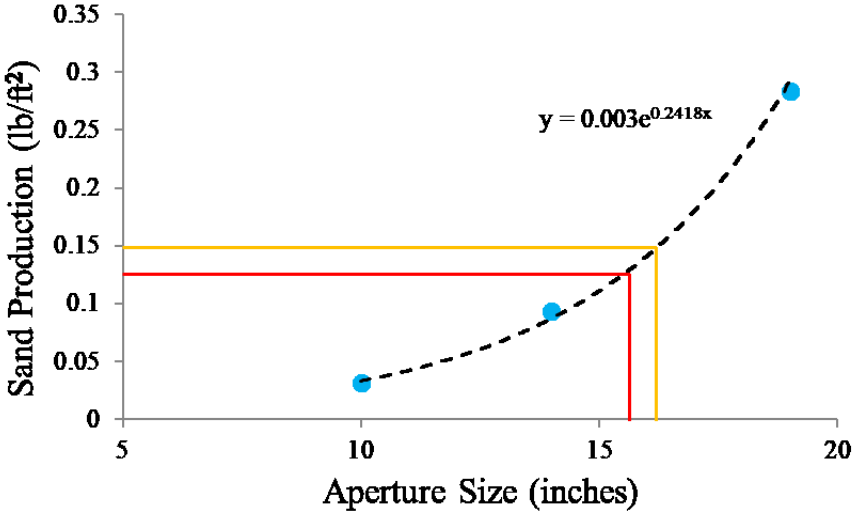

Fig.18 Sand production data points versus aperture sizes (DC-I normal condition)

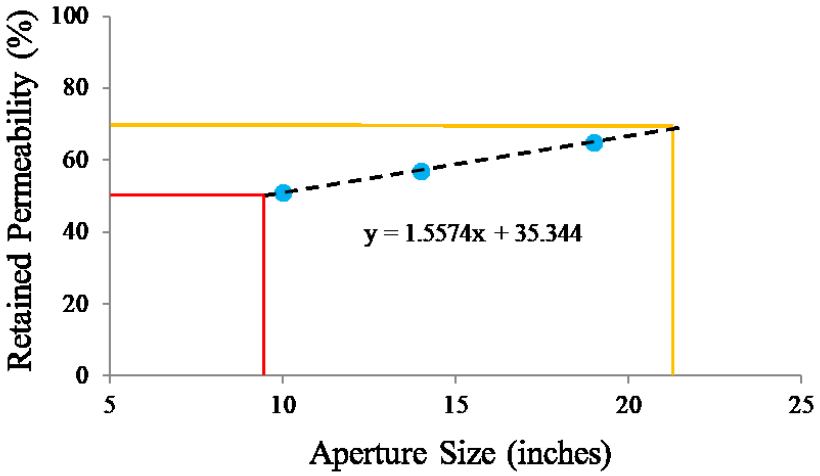

Fig. 19 Retained permeability data versus aperture sizes (DC-I normal condition)

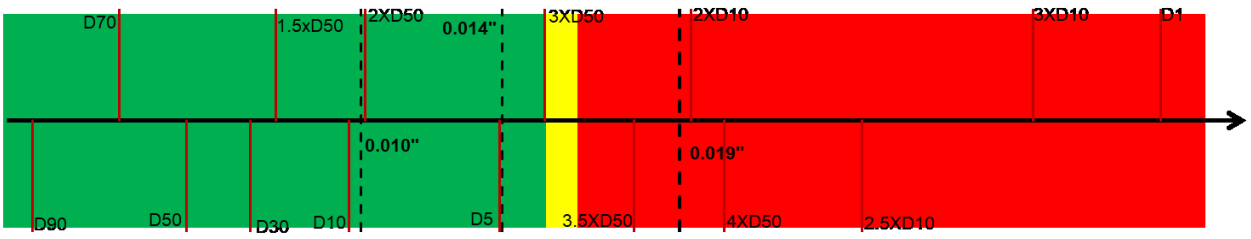

Fig. 20 Traffic light bar for sand production for DC-I (normal condition)

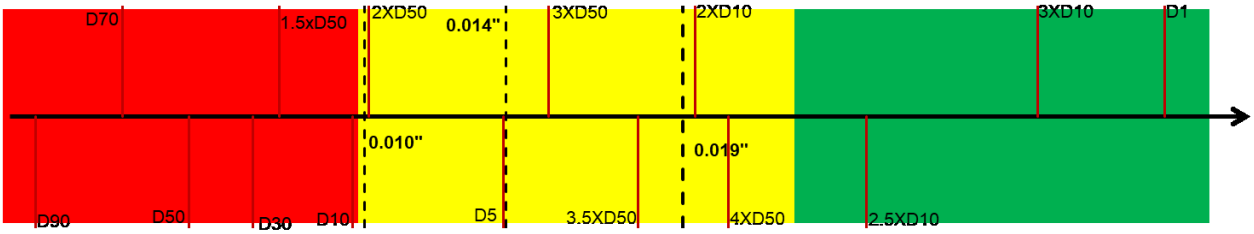

Fig. 21 Traffic light bar for retained permeability for DC-I (normal condition)

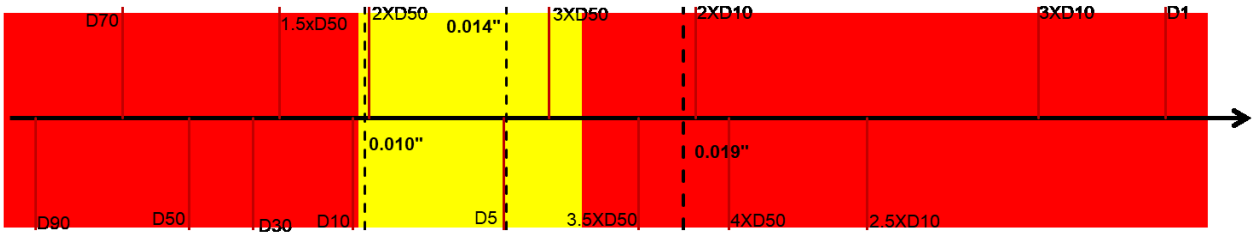

Fig. 22 Overall traffic light system of safe size window for DC-I (normal condition)

Following the abovementioned procedure, the overall graphical aperture size design criteria for all three PSD's are presented in Figures 23 through 25 under normal SAGD operation condition. Figures 26 through 28 present the overall graphical aperture size design criteria under aggressive SAGD operation conditions.

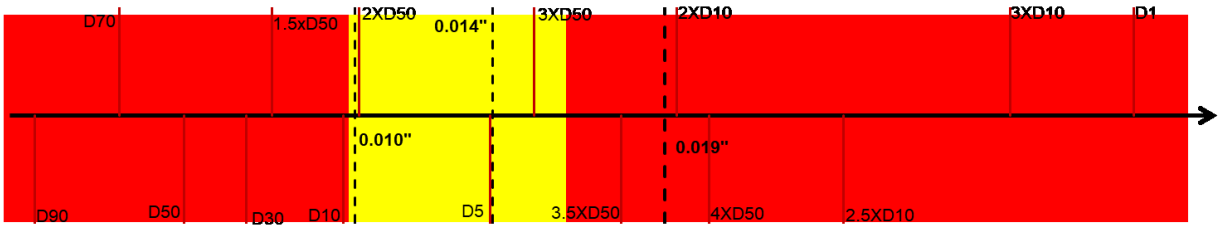

Fig. 23 Traffic light system of safe size window for DC-I (normal condition)

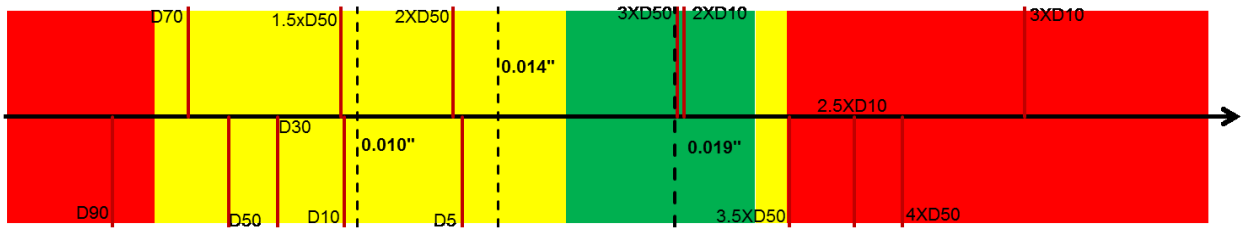

Fig. 24 Traffic light system of safe size window for DC-II (normal condition)

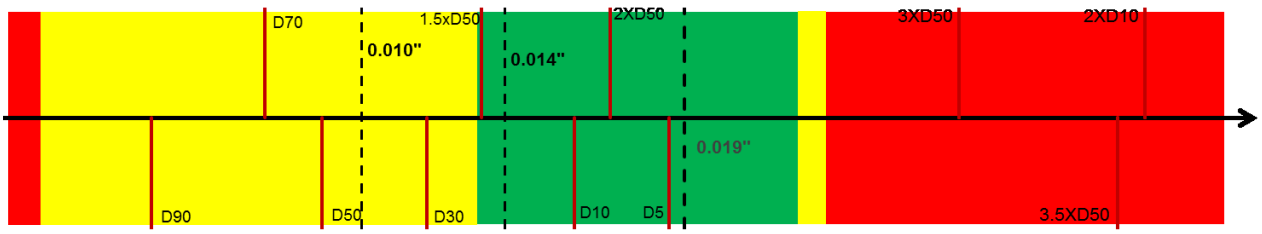

Fig. 25 Traffic light system of safe size window for DC-III (normal condition)

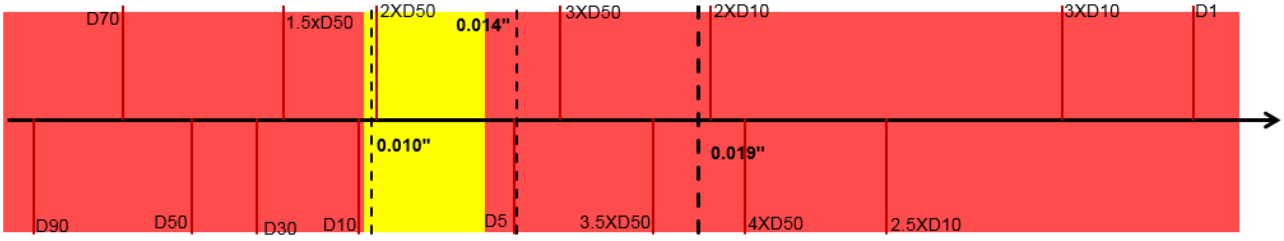

Fig. 26 Traffic light system of safe size window for DC-I (aggressive condition)

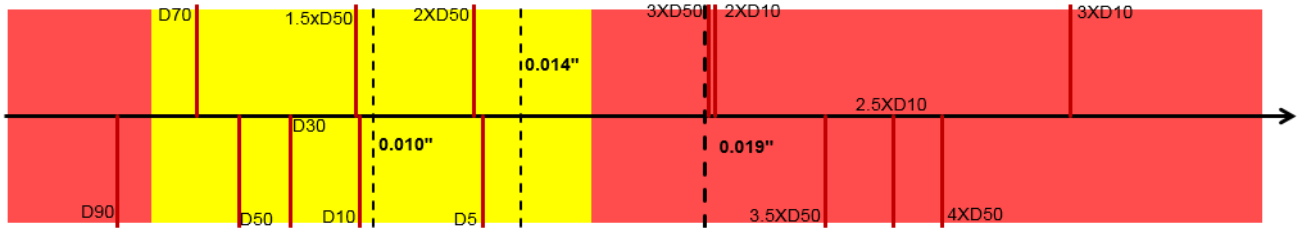

Fig. 27 Traffic light system of safe size window for DC-II (aggressive condition)

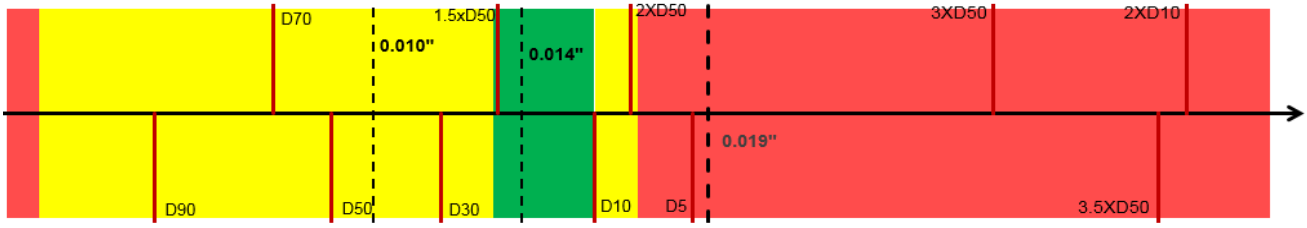

Fig. 28 Traffic light system of safe size window for DC-III (aggressive condition)

From the graphical views of the TLS criteria in Figures 23 to 25, it is evident that DC-III provides the widest safe aperture window compared to DC-I and II. This is expected as DC-III is the coarsest PSD here with the least fines content. The coarse sand in DC-III results in more stable sand bridges behind the screen apertures compared to DC-I and II for the same aperture sizes, hence, a lower amount of sand production. As such, the upper bound for DC-III TLS shifts to the right.

Also, since DC-III contains the least amount of fine particles (5.4%) compared to DC-I (14.7%) and DC-II (7.4 %), the permeability reduction due to fines migration and pore plugging is mitigated resulting in higher retained permeability values. Therefore, the small amount of sand production and higher retained permeability values for the same aperture size in DC-III yield a larger upper

bound for the sand production and a smaller lower bound for the retained permeability. In other words, DC-III can have the same sanding performance with larger aperture size and same flow performance with a smaller aperture size compared to DC-I and II. Therefore, for DC-III PSD, a larger aperture size can be selected, which can provide better flow performance without sacrificing the sanding performance.

A comparison of the TLS between normal and aggressive conditions for all three PSDs shows that the upper bound for the aggressive condition is smaller. This is due to the additional sand production caused by the steam breakthrough. The higher amount of sand production leads to a smaller lower bound to maintain desirable sanding performance.

For the field application, the TLS results show no green zone for DC-I, which means PS could not provide optimal performance for DC-I. The high fines content in DC-I results in a high level of fines migration and pore plugging in the formation. However, in formations with fewer fines content (DC-II and DC-III), the PS can provide optimal performance indicated by the existence of the green zone. Therefore, it is recommended to utilize the PS only in formations with low fines content.

5. Conclusion

This study generates an optimal size selection protocol for PS in SAGD production wells. The protocol is presented graphically by using the TLS that displays the safe size window for each PSD. The safe size window aims at keeping the produced sand within an acceptable range while reducing the plugging potential. The study incorporates not only different formation PSD data but also different reservoir and operational conditions. The pre-packed SRT facility is employed to conduct experimental tests to develop this size selection protocol. The pre-pack SRT facility allows emulating the collapsed down-hole formation condition.

The proposed protocol incorporates the PSD, reservoir conditions, fluid conditions, and flow rates as crucial factors in the size design. Results indicate satisfactory performance for the PS in clean-sand reservoirs. However, plugging potentials are found to be high for formations with high fines content. Also, sanding potential is found to be high for finer sand formations during the steam breakthrough incidents.

Finally, it is noted that some assumptions limit the present work. For example, the oil used in tests is mineral oil. However, in SAGD production wells, emulsified fluid is the dominant type of produced liquid. Also, the impacts of phenomena such as scaling, corrosion, and asphaltene precipitation are not incorporated into the testing design. Temperature is another factor neglected in this work. Further research is needed to understand the impact of these parameters on the aperture design criteria. Also, field data would be essential to validate the proposed design criteria.

Nomenclature

q_{water}: water flow rate

k_{eff}: effective permeability

A: area

ΔP_{screen}: pressure differential in the near-screen zone

μ_{water}: water viscosity

L: length

k_{abs}: absolute permeability

k_{rw}: water relative permeability

RP: retained permeability

Acknowledgment

The authors would like to acknowledge RGL Reservoir Management Inc. for providing funding and technical support to this project. Also, the authors acknowledge the Natural Sciences and Engineering Research Council of Canada (NSERC) for their financial support.

Reference

Abram, M. and Cain, G. (2014). Particle-Size Analysis for the Pike 1 Project, McMurray Formation. Journal of Canadian Petroleum Technology, 53(06), 339-354.

Al-Awad, M.N., El-Sayed, A., Desouky, S., 1999. Factors affecting sand production from unconsolidated sandstone Saudi oil and gas reservoir. Journal of King Saud University, Engineering Sciences. 11(1), 151-174.

Anderson, M., 2017. SAGD sand control: large scale testing results. In: Paper Presented at the SPE Canada Heavy Oil Technical Conference, Calgary, Alberta, Canada, 15-16 February, SPE-185967-MS.

Ballard, T., Beare, S.P., 2006. Sand retention testing: the more you do, the worse it gets. In: Paper Presented at the SPE International Symposium and Exhibition on Formation Damage Control, Lafayette, Louisiana, USA, 15-17 February, SPE-98308-MS.

Bennett, C., Gilchrist, J.M., Pitoni, E., Burton, R.C., Hodge, R.M., Troncoso, J., Ali, S.A., Dickerson, R., Price-Smith, C., Parlar, M., 2000. Design methodology for selection of horizontal open-hole sand control completions supported by field case histories. In: Paper Presented at the SPE European Petroleum Conference, Paris, France, 24-25 October. SPE-65140-MS.

Bennion, D.B., Gupta, S., Gittins, S., Hollies, D., 2009. Protocols for slotted liner design for optimum sagd operation. Journal of Canadian Petroleum Technology. 48(11), 21-26.

Birks, J., Fennell, J., Yi, Y., Gibson, J. Moncur, M. 2017. Regional geochemistry study for the Southern Athabasca Oil Sands (SAOS) area. Submitted To COSIA Hydrogeology Working Group.

Butler, R., 1985. A new approach to the modelling of steam-assisted gravity drainage. Journal of Canadian Petroleum Technology. 24(03), 42-51.

Butler, R., 1998. SAGD comes of AGE!. Journal of Canadian Petroleum Technology. 37(07), 9-12.

Butler, R., Stephens, D. 1981. The gravity drainage of steam-heated heavy oil to parallel horizontal wells. Journal of Canadian Petroleum Technology, 20(02), 90-96.

Butler, R.M., 2001. Some recent developments in SAGD. Journal of Canadian Petroleum Technology. 40(01), 18-22.

Changyin, D.O.N.G., ZHANG, Q., Kaige, G.A.O., Kangmin, Y.A.N.G., Xingwu, F.E.N.G. and Chong, Z.H.O.U., 2016. Screen sand retaining precision optimization experiment and a new empirical design model. Petroleum Exploration and Development, 43(6), pp.1082-1088.

Chanpura, R.A., Fidan, S., Mondal, S., Andrews, J.S., Martin, F., Hodge, R.M., Ayoub, J.A., Parlar, M. and Sharma, M.M., 2012a. New analytical and statistical approach for estimating and analyzing sand production through wire-wrap screens during a sand-retention test. SPE Drilling & Completion. 27(03): 417-426.

Chanpura, R.A., Hodge, R.M., Andrews, J.S., Toffanin, E.P., Moen, T., Parlar, M., 2011. A review of screen selection for applications and a new methodology. SPE Drilling & Completion. 26(01), 84-95.

Chanpura, R.A., Mondal, S., Andrews, J.S., Mathisen, A.M., Ayoub, J.A., Parlar, M., Sharma, M.M., 2012b. Modeling of square mesh screens in slurry test conditions for screen applications. In: Paper Presented at the SPE International Symposium and Exhibition on Formation Damage Control, Lafayette, Louisiana, USA,15-17 February, SPE-151637-MS.

Coberly, C., 1937. Selection of screen openings for unconsolidated sands. In: Paper Presented at the Drilling and Production Practice, New York, 1 January, API-37-189.

Constien, V.G. and Skidmore, V., 2006. screen selection using performance mastercurves. PE International Symposium and Exhibition on Formation Damage Control, Lafayette, Louisiana, USA, 15-17 February, SPE-98363-MS.

Cowie B. R., James, B., Mayer B. 2015. Distribution of total dissolved solids in McMurray Formation water in the Athabasca Oil Sands Region, Alberta, Canada: implications for regional hydrogeology and resource development. AAPG Bulletin. 99(1): 77–90.

Dang, C.T.Q., Nguyen, N.T.B., Bae, W., Nguyen, H.X., Tu, T., Chung, T., 2010. Investigation of SAGD recovery process in complex reservoir. In: Paper Presented at the SPE Asia Pacific Oil and Gas Conference and Exhibition, Brisbane, Queensland, Australia, 18-20 October, SPE-133849-MS.

Denney, D., 2008. Near-wellbore modeling: sand-production issues. Journal of Petroleum Technology. 60(09), 106-111.

Devere-Bennett, N., 2015. Using prepack sand-retention tests (SRT's) to narrow down liner/screen sizing in sagd wells. In: Paper Presented at the SPE Thermal Well Integrity and Design Symposium, Banff, Alberta, Canada, 23-25 November, SPE-178443-MS.

Dong, C., Li, Y., Zhang, Q., Feng, S., Zhang, L. 2014,. Experimental Study on Sand-Carrying Mechanism and Capacity Evaluation in Water-Producing Gas Wells and Its Application in Artificial Lift Optimization. Society of Petroleum Engineers. doi:10.2118/173700-MS

Fattahpour, V., Mahmoudi, M., Wang, C., Kotb, O., Roostaei, M., Nouri, A., Fermaniuk, B., Sauve, A., Sutton, C., 2018. Comparative study on the performance of different stand-alone sand control screens in thermal wells. In: Paper Presented at the SPE International Conference and Exhibition on Formation Damage Control, Lafayette, Louisiana, USA, 7-9 February, SPE-189539-MS.

Gates, I.D., Kenny, J., Hernandez-Hdez, I.L., Bunio, G.L., 2005. Steam injection strategy and energetics of steam-assisted gravity drainage. SPE Reservoir Evaluation & Engineering. 10(01), 19-34.

Gillespie, G., Deem, C.K., Malbrel, C., 2000. Screen selection for sand control based on laboratory tests. In: Paper Presented at the SPE Asia Pacific Oil and Gas Conference and Exhibition, Brisbane, Australia, 16-18 October, SPE-64398-MS.

Han, D.-H., Yao, Q., Zhao, H.-Z., 2007. Complex properties of heavy oil sand. In: Paper Presented at the 2007 SEG Annual Meeting, San Antonio, Texas, 23-28 September, SEG-2007-1609.

Hodge, R.M., Burton, R.C., Constien, V., Skidmore, V., 2002. An evaluation method for screen-only and gravel-pack completions. In: Paper Presented at the international Symposium and Exhibition on Formation Damage Control, Lafayette, Louisiana, 20-21 February, SPE-73772-MS.

Khilar, K.C., Fogler, H.S., 1984. The existence of a critical salt concentration for particle release. Journal of Colloid and Interface Science. 101(01), 214-224.

Kotylar, L.S., Sparks, B.D., Schutfe R., 1996. Effect of salt on the flocculation behavior of nano particles in oil sands fine tailings. Clays and Clay Minerals. 44(0l): 121-131.

Ma., C., Deng., J., Tan., Q., Li, C., Lin., H., Li, H., Liu., W. 2018. Development of a New Pre-Packed Sand-Retaining Cell. American Rock Mechanics Association.

Ma, C., Deng, J., Dong, X., Sun, D., Feng, Z., Yan, X., Hui, C. and Tian, D., 2019a. Comprehensive experimental study on the sand retention media of pre-filled sand control screens. Particulate Science and Technology, pp.1-10.

Ma, C., Deng, J., Dong, X., Sun, D., Feng, Z., Luo, C., Xiao, Q. and Chen, J., 2019b. A new laboratory protocol to study the plugging and sand control performance of sand control screens. Journal of Petroleum Science and Engineering, p.106548.

Mahmoudi, M., Fattahpour, V., Nouri, A., Rasoul, S., Yao, T., Baudet, B.A., Leitch, M., Soroush, M., 2016a. Investigation into the use of commercial sands and fines to replicate oil sands for large-scale sand control testing. In: Paper Presented at the SPE Thermal Well Integrity and Design Symposium, Banff, Alberta, Canada, 28 November-1 December, SPE-182517-MS.

Mahmoudi, M., Fattahpour, V., Nouri, A., Yao, T., Baudet, B.A., Leitch, M., Fermaniuk, B., 2016b. New criteria for slotted liner design for heavy oil thermal production. In: Paper Presented at the SPE Thermal Well Integrity and Design Symposium, Banff, Alberta, Canada, 28 November-1 December, SPE-182511-MS.

Mahmoudi, M. (2017). New Sand Control Design Criteria and Evaluation Testing for Steam Assisted Gravity Drainage (SAGD) Wellbores (Doctoral dissertation, Doctoral Thesis, University of Alberta (March 2017)).

Mahmoudi, M., Fattahpour, V., Velayati, A., Roostaei, M., Kyanpour, M., Alkouh, A., Sutton, C., Fermaniuk, B., Nouri, A., 2018. Risk assessment in sand control selection: introducing a traffic light system in stand-alone screen selection. In: Paper Presented at the SPE International Heavy Oil Conference and Exhibition, Kuwait City, Kuwait, 10-12 December, SPE-193697-MS.

Matanovic, D., Cikes, M., Moslavac, B., 2012. Sand control in well construction and operation. First Edition: Springer-Verlag Berlin Heidelberg.

Mathisen, A.M., Aastveit, G.L., Alteraas, E., 2007. Successful installation of stand alone sand screen in more than 200 wells-the importance of screen selection process and fluid qualification. In: Paper Presented at the European Formation Damage Conference, Scheveningen, The Netherlands, 30 May-1 June, SPE-107539-MS.

Minnich, K.R., Gamache, D.E. and Kus, J., Statoil Canada Ltd, Veolia Water Solutions and Technologies North America Inc, 2013. Process for solidifying organic and inorganic

provisional constituents contained in produced water from heavy oil operations. U.S. Patent 8,506,467.

Montero Pallares, J.D., Chissonde, S., Kotb, O., Wang, C., Roostaei, M., Nouri, A., Mahmoudi, M., Fattahpour, V., 2018a. A critical review of sand control evaluation testing for sagd applications. In: Paper Presented at the SPE Canada Heavy Oil Technical Conference, Calgary, Alberta, Canada, 13-14 March, SPE-189773-MS.

Montero Pallares, J.D., Wang, C., Haftani, M., Pang, Y., Mahmoudi, M., Fattahpour, V., Nouri, A., 2018b. Experimental assessment of wire-wrapped screens performance in SAGD production wells. In: Paper Presented at the SPE Thermal Well Integrity and Design Symposium, Banff, Alberta, Canada, 27-29 November, SPE-193375-MS.

Naganathan, S., Li, P. Y., Hong, L. H., & Sharara, A. M. (2006, January 1). Developing Heavy Oil Fields By Horizontal Well Placement - A Case Study. Society of Petroleum Engineers. doi:10.2118/104163-MS

Nasr, T., Golbeck, H., Pierce, G., 1998. SAGD operating strategies. In: Paper Presented at the SPE International Conference on Horizontal Well Technology, Calgary, Alberta, Canada, 1-4 November, SPE-50411-MS.

Noik, C., Dalmazzone, C. S. H., Goulay, C., & Glenat, P. (2005, January 1). Characterisation and Emulsion Behaviour of Athabasca Extra Heavy Oil Produced by SAGD. Society of Petroleum Engineers. doi:10.2118/97748-MS

O'Hara, M., 2015. Thermal operations in the McMurray; an approach to sand control. In: Paper Presented at the SPE Thermal Well Integrity and Design Symposium, Banff, Alberta, Canada, 23-25 November, SPE-178446-MS.

RGL Reservoir Management Inc, 2018 Retrieved from https://www.rglinc.com/solutions/sand-control/propunch/

Romanova, U.G., Gillespie, G., Sladic, J., Ma, T., Solvoll, T.A., Andrews, J.S., 2014. A comparative study of wire wrapped screens vs. slotted liners for steam assisted gravity drainage operations. In: Paper Presented at the In World Heavy Oil Congress, New Orleans, March 5-7, WHOC14-113

Romanova, U.G., Ma, T., 2013. An investigation on the plugging mechanisms in a slotted liner from the steam assisted gravity operations. In: Paper Presented at the SPE European Formation Damage Conference & Exhibition, Noordwijk, The Netherlands, 5-7 June, SPE-165111-MS.

Romanova, U.G., Ma, T., Piwowar, M., Strom, R., Stepic, J., 2015. Thermal formation damage and relative permeability of oil sands of the Lower Cretaceous Formations in Western Canada. In: Paper Presented at the SPE Canada Heavy Oil Technical Conference, Calgary, Alberta, Canada, 9-11 June, SPE-174449-MS.

Sanyal, T., Al-Hamad, K., Jain, A.K., Al-Haddad, A.A., Kholosy, S., Ali, M.A., Sennah, A., Farag, H., 2012. Laboratory challenges of sand production in unconsolidated cores. In: Paper Presented at the SPE Kuwait International Petroleum Conference and Exhibition, Kuwait City, Kuwait, 10-12 December, SPE-163275-MS.

Spronk, E.M., Doan, L.T., Matsuno, Y., Harschnitz, B., 2015. SAGD liner evaluation and liner test design for JACOS Hangingstone SAGD development. In: Paper Presented at the SPE Canada Heavy Oil Technical Conference, Calgary, Alberta, Canada, 9-11 June, SPE-174503-MS.

Underdown, D.R., Dickerson, R.C., Vaughan, W., 2001. The nominal sand-control screen: a critical evaluation of screen performance. SPE Drilling & Completion. 16(04), 252-260.

Wang, C., Pang, Y., Montero Pallares, J.D., Haftani, M., Fattahpour, V., Mahmoudi, M., Nouri, A., 2018. Impact of anisotropic stresses on the slotted liners performance in steam assisted gravity drainage process. In: Paper Presented at the SPE Thermal Well Integrity and Design Symposium, Banff, Alberta, Canada, 27-29 November, SPE-193347-MS.

Wang, C., Pang, Y., Mahmoudi, M., Haftani, M., Salimi, M., Fattahpour, V. and Nouri, A., 2020a. A set of graphical design criteria for slotted liners in steam assisted gravity drainage production wells. Journal of Petroleum Science and Engineering, p.106608.

Wang, C., Pang, Y., Montero Pallares, J., Haftani, M., and Nouri, A., 2020b. Developing a methodology to characterize formation damage (pore plugging) due to fines migration in sand control tests. Journal of Petroleum Science and Engineering, p.106793.

Williams, C.F., Richard, B.M., Horner, D., 2006. A new sizing criterion for conformable and nonconformable sand screens based on uniform pore structures. In: Paper Presented at the SPE International Symposium and Exhibition on Formation Damage Control, Lafayette, Louisiana, USA, 15-17 February, SPE-98235-MS.

Xie, J., 2015. Slotted liner design optimization for sand control in SAGD wells. In: Paper Presented at the SPE Thermal Well Integrity and Design Symposium, Banff, Alberta, Canada, 23-25 November, SPE-178457-MS.

Yi, X., 2002. Simulation of sand production in unconsolidated heavy oil reservoirs. Journal of Canadian Petroleum Technology. 41(03), 11-13.

Zhang W., Youn S., Doan, Q.T., 2007. Understanding reservoir architectures and steam-chamber growth at Christina Lake, Alberta, by using 4D seismic and crosswell seismic imaging. SPE Reservoir Evaluation & Engineering. 10(05), 446-452.

Zhang, Z. (2017). An Advanced Sand Control Technology for Heavy Oil Reservoirs (Doctoral dissertation, University of Calgary).